ISSN 1070-3284, Russian Journal of Coordination Chemistry, 2015, Vol. 41, No. 4, pp. 247–254. © Pleiades Publishing, Ltd., 2015.

Hydrothermal Syntheses, Crystal Structures, and Magnetic Properties of Three Manganese(II) Complexes Based on 4'-Substituted 2,2':6',2''-Terpyridine Ligands[1]

W. W. Fu*, M. S. Chen, W. Li, Y. Liu, F. X. Zhang, and D. Z. Kuang

Key Laboratory of Functional Organometallic Materials of Hunan Province College, Department of Chemistry and Materials Science, Hengyang Normal University, Hengyang, 421008 P.R. China

**e-mail: w.w.fu@hotmail.com*

Received September 11, 2014

Abstract—Three manganese coordination compounds, $[Mn(Meophtpy)_2] \cdot 2ClO_4$ (Meophtpy = 4'-(4-methoxylphenyl)-2,2':6',2''-terpyridine) (**I**), $[Mn(Ftpy)_2](ClO_4)_2$ (Ftpy = 4'-(2-furyl)-2,2':6',2''-terpyridine) (**II**) and $[Mn(m\text{-}ClPhtpy)_2] \cdot 2ClO_4$ (*m*-ClPhtpy = 4'-(3-chlorophenyl)-2,2':6',2''-terpyridine) (**III**), have been synthesized by hydrothermal methods and characterized by IR, elemental analysis, powder and single-crystal X-ray diffraction analyses (CIF files CCDC nos. 945032 (**I**), 945033 (**II**), 945034 (**III**)). In most cases, the face-to-face interactions between pyridyl rings or phenyl rings facilitate the construction of 3D network in the crystal for all three complexes. The magnetic properties of three complexes have been investigated.

DOI: 10.1134/S1070328415040028

INTRODUCTION

Coordination compounds based on 2,2':6',2''-terpyridine have been widely investigated for their diverse structures and potential applications in luminescence, magnetism, catalysis, biology and nonlinear optical properties [1–7]. Among these explorations, one of the most used strategy is to fine tune these properties by adjusting the substitution group on 4' position of 2,2':6',2''-terpyridine [1, 8–11]. Manganese(II) complexes have been well researched for magnetic properties [12–14]. Although many 2,2':6',2''-terpyridine coordinated manganese compounds have been researched [15–18], only a few of them have been investigated for their magnetic properties [4, 19, 20]. In order to test the influence of different substitutes on the crystal packing and magnetic properties, in this paper, three new manganese(II) complexes based on different 4'-substituted 2,2':6',2''-terpyridines have been synthesized and their magnetic properties have been studied. To the best of our knowledge, compounds constructed of 4'-(2-furyl)-2,2':6',2''-terpyridine (Ftpy) and 4'-(3-chlorophenyl)-2,2':6',2''-terpyridine (*m*-ClPhtpy) were first been reported.

EXPERIMENTAL

Materials and methods. All reagents and solvents were commercially available and used as received. Elemental analyses were carried out on EA1110 CHNS-0 CE elemental analyzer. Fourier-transform infrared spectra (FT–IR) were recorded on a Shimadzu Prestige-21 FT–IR spectrometer using dry KBr pellets from 400–4000 cm^{-1}. The temperature-dependent magnetic susceptibilities were measured with crystalline samples on a Quantum Design MPMS XL-5 Squid magnetometer in a magnetic field of 1000 Oe from 2 to 300 K. Power X-ray diffraction (PXRD) measurements were performed on a Bruker D8 diffractometer operated at 40 kV and 40 mA using CuK_α radiation (λ = 1.5418 Å).

Synthesis of $[Mn(Meophtpy)_2] \cdot 2ClO_4$ (I). Meophtpy (0.034 g, 0.1 mmol), $MnSO_4 \cdot H_2O$ (0.0085 g, 0.05 mmol) and $NaClO_4$ (0.012 g, 0.1 mmol) were mixed in water (5 mL) and ethanol (5 mL) and sealed in a 16 mL Teflon-lined stainless steel vessel. After heating at 160°C for 72 h, the temperature was gradually dropped to room temperature. Brown block crystals were obtained, washed with water and dried in air.

For $C_{44}H_{34}N_6O_{10}Cl_2Mn$			
anal. calcd., %:	C, 56.67;	H, 3.67;	N, 9.01.
Found, %:	C, 56.53;	H, 3.71;	N, 8.95.

IR (KBr; ν, cm^{-1}): 3080 m, 2938 m, 2843 m, 2017 w, 1601 v.s, 1572 s, 1547 s, 1518 s, 1477 s, 1431 s, 1406 s, 1244 s, 1184 s, 1090 v.s, 1014 s, 885 m, 829 s, 791 s,

[1] The article is published in the original.

748 m, 729 m, 688 m, 658 m, 638 m, 623 s, 577 m, 523 m, 407 m.

Synthesis of $[Mn(Ftpy)_2] \cdot 2ClO_4$ (II) was similar to that of **I** except that Ftpy (0.030 g, 0.1 mmol) was used instead of Meophtpy.

For $C_{38}H_{28}N_6O_{11}Cl_2Mn$

anal. calcd., %:	C, 52.43;	H, 3.24;	N, 9.65.
Found: %:	C, 52.04;	H, 3.30;	N, 9.57.

IR (KBr; ν, cm^{-1}): 3588 s, 3526 s, 3109 m, 3074 m, 1614 v.s, 1600 v.s, 1570 s, 1545 s, 187 s, 1475 s, 1458 s, 1431 s, 1383 m, 1304 w, 1252 m, 1230 m, 1090 v.s, 1014 v.s, 928 m, 883 m, 833 m, 793 s, 758 m, 744 s, 729 s, 685 m, 623 s, 584 m, 474 m, 447 m, 407 m.

Synthesis of $[Mn(m\text{-}ClPhtpy)_2] \cdot 2ClO_4$ (III) was similar to that of **I** except that *m*-ClPhtpy (0.034 g, 0.1 mmol) was used instead of Meophtpy.

For $C_{42}H_{28}N_6O_8Cl_4Mn$

anal. calcd., %:	C, 53.58;	H, 3.00;	N, 8.93.
Found,%:	C, 53.44;	H, 2.97;	N, 8.89.

IR (KBr; ν, cm^{-1}): 3073 m, 1612 v.s, 1600 v.s, 1570 m, 1547 s, 1474 s, 1435 m, 1418 m, 1398 s, 1362 w, 1300 w, 1248 m, 1163 m, 1090 v.s, 1014 s, 868 m, 781 s, 744 m, 723 m, 685 m, 658 m, 623 s, 523 m, 409 m.

X-ray crystallography. Crystals of **I**–**III** were mounted on a Bruker SMART APEX II CCD diffractometer with graphite monochromated MoK_α radiation (λ = 0.71073 Å) at 123 K. Empirical absorption corrections were applied by using the SADABS program. The structures were solved by direct methods and refined by full-matrix least squares on F^2 via SHELXL-97 program [21]. All non-hydrogen atoms were refined anisotropically and the hydrogen atoms were generated geometrically. Crystallographic data and structural refinement parameters for compounds **I**–**III** are listed in Table 1. Selected bond lengths and angles are presented in Table 2.

Supplementary material has been deposited with the Cambridge Crystallographic Data Centre (CCDC nos. 945032 (**I**), 945033 (**II**), 945034 (**III**); deposit@ccdc.cam.ac.uk or http://www.ccdc.cam.ac.uk).

RESULTS AND DISCUSSION

The asymmetric unit of **I** contains one Mn^{2+} cation, two Meophtpy ligands and two perchlorate anions. The manganese(II) ion is coordinated by six N atoms from two Meophtpy ligands. The distances between Mn and N from central pyridines (Mn–N(1) and Mn–N(4)) are 2.206(2) and 2.209(2) Å which are slightly shorter than that between Mn and N from outer pyridines (Mn–N(2), Mn–N(6), Mn–N(3), and Mn–N(5) 2.240(2), 2.242(2), 2.242(2), and 2.270(2) Å). Three transoid angles are: N(1)MnN(4) 167.12(8)°, N(2)MnN(3) 143.20(8)°, and N(5)MnN(6) 143.90(9)°, and the other twelve cisoid angles are ranging from 71.78(8)° to 120.69(9)°. Both the differences of bond lengths and bond angles show a distorted octahedral geometry in **I** which are common for terpyridine coordinated compounds [22, 23]. The angles between phenyl ring and terpyridine ring are 19.6° and 7.9°. The angle between two terpyridine rings is 73.1° which are deviated from right angle.

Eleven hydrogen bonds all with C–H···O type link the individual components in **I** into three dimensional network which have been shown in Fig. 1b and Table 3. Except for O(8), all O atoms on perchlorate anions are acceptors with hydrogen on C as donors. The O(3) atom is triple acceptor linked with hydrogens H(8), H(16) and H(44*C*) which are attached to C(8), C(16), and C(44). The O(4) and O(7) atoms are double acceptors with hydrogen H(7), H(32), and H(10), H(22*A*) which are attached to C(7), C(32), and C(10), C(22), respectively. The most shortest hydrogen bonds (H···O) are 2.33 Å for C(7)–H(7)···O(4)^{i} and C(35)–H(35)···O(10)^{vi}. The other moderate hydrogen bonds are 2.39 Å for C(32)–H(32)···O(4)^{v}, 2.41 Å for C(10)–H(10)···O(7)^{ii}, and 2.46 Å for C(22)–H(22*A*)···O(7)^{iii} (symmetry codes are shown in Table 3). All the other hydrogen bond lengths are longer than 2.51 Å, and they are weak hydrogen bonds.

There exist five kinds of offset face-to-face interactions between pyridine and benzene rings as that shown in Fig. 1c. The distance between centroids of outer pyridine rings is 3.824 Å showing moderate interaction. The distance between centroids of pyridine ring (N(5), C(33)–C(37)) and benzene ring (C(38)–C(43)) are 3.924 Å showing moderate interaction too. The other three π–π interactions are relevant with benzene ring (C(16)–C(21)), two with pyrdidine ring (N(2), C(6)–C(10); N(3), C(11)–C(15)) of 4.483 and 4.617 Å, respectively, and the third with benzene ring (C(38)–C(43)) of 4.724 Å showing weak interactions.

The asymmetric unit of **I** contains one Mn^{2+} cation, two Ftpy ligands, two perchlorate anions and one water molecule. The manganese(II) ion is coordinated by six N atoms from two Ftpy ligands. The distances between Mn and N from central pyridines (Mn–N(1) and Mn–N(4)) are 2.1914(14) and 2.1864(14) Å which are slightly shorter than that between Mn and N from outer pyridines (Mn–N(2), Mn–N(6), Mn–N(3), and Mn–N(5)), 2.2530(14), 2.2340(15), 2.2242(14), and 2.2844(14) Å. These six Mn–N bond lengths are shorter than that in **I** except for Mn–N(5). Three transoid angles, N(1)MnN(4), N(2)MnN(3), and N(5)MnN(6), are 165.09(5)°, 143.95(5)°, and 145.18(5)°, respectively, and other twelve cisoid angles are ranging from 72.41(5)° to 119.03(5)°. All these fifteen bond angles are similar with that in **I**. Both the differences of bond lengths and bond angles show a distorted octahedral geometry in

Table 1. Crystal data and structure refinement parameters for **I**–**III**[a]

Parameter	Value		
	I	**II**	**III**
Formula mass	932.61	870.50	941.44
Crystal system	Monoclinic	Triclinic	Orthorhombic
Space group	$P2_1/c$	$P\bar{1}$	$Pcca$
a, Å	18.1425(13)	10.4081(7)	24.6383(14)
b, Å	15.2934(11)	11.3866(8)	10.8645(6)
c, Å	16.2992(11)	16.0693(11)	14.9919(8)
α, deg	90	97.6000(10)	90
β, deg	113.3580(10)	102.8290(10)	90
γ, deg	90	93.2150(10)	90
V, Å^3	4151.8(5)	1833.4(2)	4013.1(4)
Z	4	2	4
ρ_{calcd}, g/cm^3	1.492	1.577	1.558
μ, mm^{-1}	0.515	0.579	0.659
F(000)	1916	890	1916
θ, deg	1.81–25.01	1.31–28.32	1.65–25.01
Reflections collected/independed	23072/7318	13231/8973	43923/3536
R_{int}	0.0469	0.0144	0.0763
GOOF on F^2	1.105	1.069	1.071
Parameters refined	564	523	296
R, wR_2 ($I > 2\sigma(I)$)*	0.0509, 0.1663	0.0363, 0.0932	0.0518, 0.1255
R, wR_2 (all data)*	0.0571, 0.1731	0.0457, 0.0976	0.0594, 0.1337
Largest diff. peak and hole, e/Å^3	1.557 and –1.016	0.482 and –0.604	0.656 and –0.524

* $R = \Sigma(||F_o| - F_c||)/\Sigma|F_o|$, $wR = [Sw(|F_j|^2 - |F_c|^2)^2/\Sigma w(F_o^2)]^{1/2}$.

II like **I** and other terpyridine coordinated compounds [22, 23]. The angles between furan ring and terpyridine ring planes are 7.3° and 0.9° which suggest fine coplanar properties. The mean deviation of terpyridine ring (N(1)–N(2)–N(3)) is 0.0771 Å. The angle between two terpyridine rings is 94.6° which are slightly deviated from a right angle.

Eleven hydrogen bonds, two with O–H···O type and others with C–H···O type, link the individual components in **II** into three dimensional network which have been shown in Fig. 2b and Table 3. The O(1*w*) atom is triple acceptor linked with hydrogens H(2), H(18), and H(29) which are attached with C(2), C(18), and C(29). The O(6) atom is triple acceptor too, linked with hydrogen H(1*wB*), H(8), and H(13) which are attached to O(1*w*), C(8), and C(13). The O(8) atom is double acceptor with hydrogen H(21) and H(31) attached to C(21) and C(31). The most shortest hydrogen bond is 2.18 Å for O(1*w*)–H(1*wB*)···O(6)^{ii}. The other moderate hydrogen bonds are 2.32 Å for O(1*w*)–H(1*wA*)···O(4)^{i}, 2.41 Å for C(18)–H(18)···O(1*w*)^{viii}, 2.45 Å for C(29)–H(29)···O(1*w*)^{x}, 2.47 Å both for C(2)–H(2)···O(1*w*)^{iii} and C(8)–H(8)···O(3)^{iv} (symmetry codes are shown in Table 3). All the other hydrogen bond lengths are longer than 2.51 Å, and they are weak hydrogen bonds.

There exist five offset face-to-face interactions between pyridine and benzene rings as that shown in Fig. 2c. The distances between centroids of outer pyridine rings are 3.824 Å showing strong interactions. The distances between centroids of one pyridine ring (N(5), C(33)–C(37)) and benzene ring (C(38)–C(43)) are 3.924 Å show strong interactions too. Three π–π interactions are relevant with benzene ring (C(16)–C(21)), two with pyridine ring (N(2), C(6)–C(10); N(3), C(11)–C(15)) of 4.483 and 4.617 Å and the third with benzene ring (C(38)–C(43)) of 4.724 Å showing moderate interactions.

The asymmetric unit of **III** contains one half of Mn^{2+} cation, one Ftpy ligand and two halves of perchlorate anions [24]. The manganese(II) ion is coordinated by six N atoms from two *m*-ClPhtpy ligands.

Table 2. Selected bond lengths and angles for **I**–**III***

Bond	*d*, Å	Bond	*d*, Å	Bond	*d*, Å
I		**II**		**III**	
Mn(1)–N(1)	2.206(2)	Mn(1)–N(4)	2.1864(14)	Mn(1)–N(1)	2.189(2)
Mn(1)–N(4)	2.209(2)	Mn(1)–N(1)	2.1914(14)	Mn(1)–N(2)	2.231(3)
Mn(1)–N(2)	2.240(2)	Mn(1)–N(3)	2.2242(14)	Mn(1)–N(3)	2.238(3)
Mn(1)–N(6)	2.242(2)	Mn(1)–N(6)	2.2340(15)		
Mn(1)–N(3)	2.242(2)	Mn(1)–N(2)	2.2530(14)		
Mn(1)–N(5)	2.270(2)	Mn(1)–N(5)	2.2844(14)		
Angle	ω, deg	Angle	ω, deg	Angle	ω, deg
I		**II**		**III**	
N(1)Mn(1)N(4)	167.12(8)	N(4)Mn(1)N(1)	165.09(5)	N(1)Mn(1)N(1)^{i}	167.70(13)
N(1)Mn(1)N(2)	71.78(8)	N(4)Mn(1)N(3)	116.99(5)	N(1)Mn(1)N(2)^{i}	115.93(9)
N(4)Mn(1)N(2)	110.49(8)	N(1)Mn(1)N(3)	72.86(5)	N(1)Mn(1)N(2)	72.49(9)
N(1)Mn(1)N(6)	120.69(9)	N(4)Mn(1)N(6)	72.80(5)	N(2)^{i}Mn(1)N(2)	100.92(15)
N(4)Mn(1)N(6)	72.03(9)	N(1)Mn(1)N(6)	119.03(5)	N(1)Mn(1)N(3)	72.33(9)
N(2)Mn(1)N(6)	97.01(8)	N(3)Mn(1)N(6)	95.04(5)	N(1)^{i}Mn(1)N(3)	99.25(9)
N(1)Mn(1)N(3)	72.20(8)	N(4)Mn(1)N(2)	99.02(5)	N(2)^{i}Mn(1)N(3)	91.84(10)
N(4)Mn(1)N(3)	106.30(7)	N(1)Mn(1)N(2)	72.23(5)	N(2)Mn(1)N(3)	144.71(9)
N(2)Mn(1)N(3)	143.20(8)	N(3)Mn(1)N(2)	143.95(5)	N(3)^{i}Mn(1)N(3)	96.43(14)
N(6)Mn(1)N(3)	94.83(8)	N(6)Mn(1)N(2)	94.07(5)		
N(1)Mn(1)N(5)	95.38(8)	N(4)Mn(1)N(5)	72.41(5)		
N(4)Mn(1)N(5)	71.87(8)	N(1)Mn(1)N(5)	95.52(5)		
N(2)Mn(1)N(5)	95.59(8)	N(3)Mn(1)N(5)	99.51(5)		
N(6)Mn(1)N(5)	143.90(9)	N(6)Mn(1)N(5)	145.18(5)		
N(3)Mn(1)N(5)	95.00(8)	N(2)Mn(1)N(5)	92.47(5)		

* Symmetry codes: ^{i} $-x + 1/2, -y, z$.

The distance between Mn and N from central pyridines (Mn–N(1)) is 2.189(2) Å which is slightly shorter than that between Mn and N from outer pyridines (Mn–N(2) and Mn–N(3) 2.231(3) and 2.238(3) Å). Three transoid angles, N(1)MnN(1)^{i}, N(2)MnN(3) and N(2)^{i}MnN(3)^{i}, are 167.12(8)°, 144.71(9)° and 144.71(9)°, respectively, and the other twelve cisoid angles are ranging from 72.34(9)° to 115.93(9)° (symmetry codes are shown in Table 2). Both the differences of bond lengths and bond angles show a distorted octahedral geometry in **III** like **I** and **II**. The angle between phenyl ring and terpyridine ring is 33.3°. The angle between two terpyridine rings is 84.6° which are slightly deviated from right angle.

Four kinds of hydrogen bonds, all with C–H···O type, link the individual components in **III** into three dimensional network which have been shown in Fig. 3b and Table 3. The O(3) atom is double acceptor linked to hydrogens H(10) and H(13) which are attached to C(10) and C(13), respectively. The O(2) and O(7) atoms are linked to H(13) and H(15) with C(13) and C(15) as donors. The shortest hydrogen bond is 2.31 Å for C(10)–H(10)···O(3)^{i} showing strong interactions. The other moderate hydrogen bonds are 2.44 Å for C(13)–H(13)···O(2)^{ii}, 2.47 Å for C(13)–H(13)···O(3)^{iii}. The longest hydrogen bonds are 2.52 Å for C(15)–H(15)···O(7)^{iv} (symmetry codes are shown in Table 3).

There exist two kinds of offset face-to-face interactions all between benzene rings as that shown in Fig. 3c. The distances between centroids of benzene ring (C(16)–C(21)) and (C(16)–C(21))^{i} (symmetry code: $^{i} - x + 1/2, y, z + 1/2$) are 3.895 Å, that shows moderate interaction. The distances between centroids of benzene ring (C(16)–C(21)) and (C(16)–C(21))^{ii} (symmetry code: $^{ii} -x, -y + 1, -z + 1$) are 3.895 Å, that shows weak interaction.

We made comparison between simulated and experimental X-ray powder diffraction patterns of **I**–**III**. All the peaks observed in the measured curves approximately match the simulated curves generated from

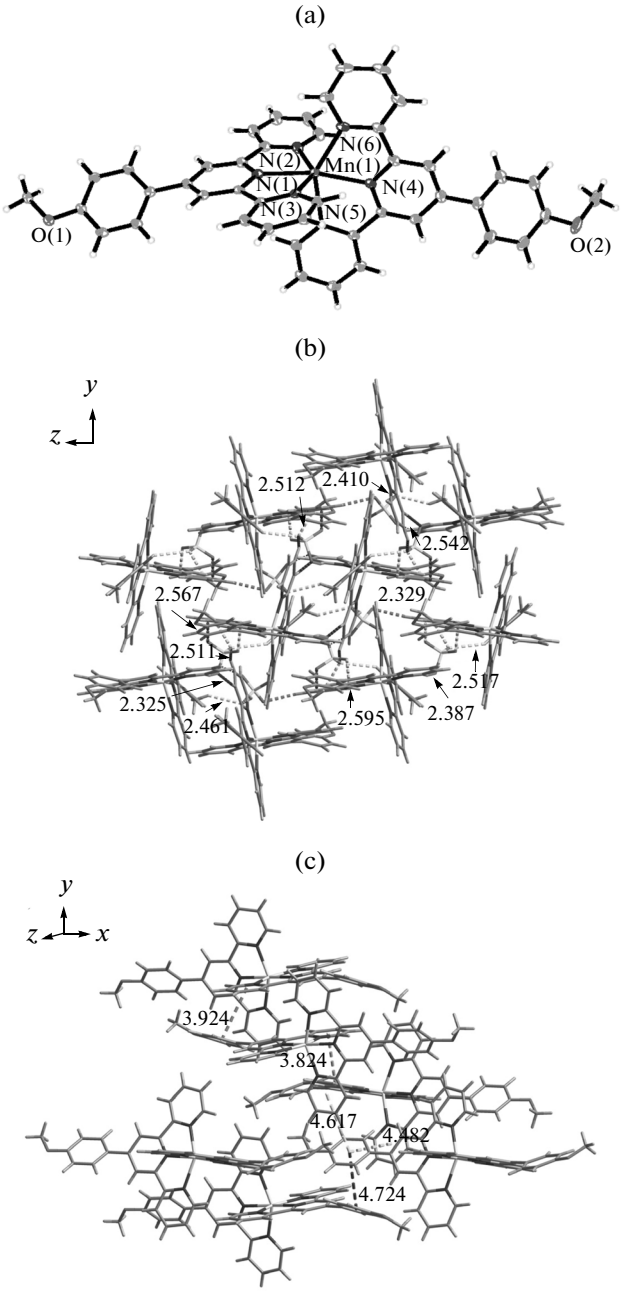

Fig. 1. The ORTEP view of $[Mn(Meophtpy)_2]^{2+}$ in **I** with thermal ellipsoids at 30% probability level (a); the 3D supramolecular network of **I** formed through hydrogen bonds (shown in dashed lines) (b); the face-to-face π–π interactions in **I** (shown in dashed lines) (c).

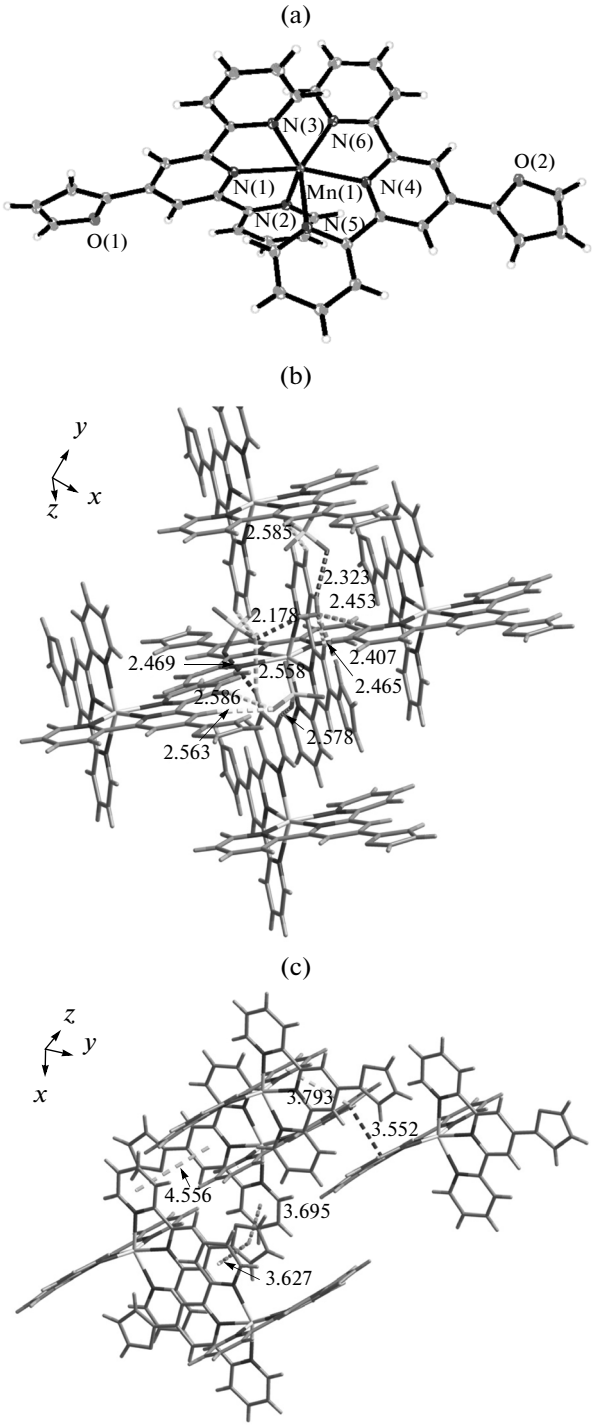

Fig. 2. The ORTEP view of $[Mn(Ftpy)_2]^{2+}$ in **II** with thermal ellipsoids at 30% probability level (a); the 3D supramolecular network of **II** formed through hydrogen bonds (shown in dashed lines) (b); the face-to-face π–π interactions in **II** (shown in dashed lines) (c).

single-crystal diffraction data, which clearly confirms the phase purity of the products.

The measurement of magnetic susceptibility for **I**–**III** in solid state were performed from 2 to 300 K under a field of 1000 Oe. The magnetic susceptibility (χ_M) and product of the susceptibility with temperature ($\chi_M T$) are shown in Fig. 4. For **I**, the $\chi_M T$ value at 300 K is 4.202 $cm^3\,mol^{-1}\,K$, slightly lower than the spin-only value of 4.375 $cm^3\,mol^{-1}\,K$ per Mn^{2+} ion ($S = 5/2$). For **II**, the $\chi_M T$ value at 300 K is 4.60051 $cm^3\,mol^{-1}\,K$. For **III**, the $\chi_M T$ value at 300 K is 4.23 $cm^3\,mol^{-1}\,K$. The

Table 3. Geometric parameters of hydrogen bonds for **I**–**III***

D–H···A	Distance, Å			Angle DHA, deg
	D–H	H···A	D···A	
		I		
C(7)–H(7)···O(4)^{i}	0.95	2.33	3.262(5)	169
C(8)–H(8)···O(3)	0.95	2.51	3.106(5)	121
C(10)–H(10)···O(7)^{ii}	0.95	2.41	3.248(4)	147
C(16)–H(16)···O(3)	0.95	2.52	3.323(5)	143
C(22)–H(22*A*)···O(7)^{iii}	0.95	2.46	3.335(4)	148
C(30)–H(30)···O(9)^{iv}	0.95	2.54	3.428(4)	155
C(32)–H(32)···O(4)^{v}	0.95	2.39	3.328(5)	171
C(35)–H(35)···O(10)^{vi}	0.95	2.33	3.260(4)	166
C(36)–H(36)···O(5)	0.95	2.57	3.297(5)	134
C(37)–H(37)···O(6)	0.95	2.60	3.160(6)	118
C(44)–H(44*C*)···O(3)^{vii}	0.98	2.51	3.439(6)	157

* Symmetry codes: ^{i} $-x, -y-1, -z$; ^{ii} $x, y-1, z$; ^{iii} $-x, y+3/2, -z+1/2$; ^{iv} $-x+1, y+3/2, -z+1/2$; ^{v} $x, -y+1/2, z-1/2$; ^{vi} $-x+1, y+3/2, -z+3/2$; ^{vii} $x+1, y, z$.

		II		
O(1*w*)–H(1*wA*)···O(4)^{i}	0.78	2.32	3.032(2)	152
O(1*w*)–H(1*wB*)···O(6)^{ii}	0.84	2.18	2.987(2)	161
C(2)–H(2)···O(1*w*)^{iii}	0.95	2.47	3.394(2)	166
C(8)–H(8)···O(3)^{iv}	0.95	2.47	3.306(2)	147
C(8)–H(8)···O(6)^{v}	0.95	2.55	3.449(2)	157
C(9)–H(9)···O(9)^{vi}	0.95	2.58	3.476(3)	158
C(13)–H(13)···O(6)^{vii}	0.95	2.58	3.426(2)	148
C(18)–H(18)···O(1*w*)^{viii}	0.95	2.41	3.325(2)	162
C(21)–H(21)···O(8)^{ix}	0.95	2.56	3.506(2)	172
C(29)–H(29)···O(1*w*)^{x}	0.95	2.45	3.356(2)	159
C(31)–H(31)···O(8)^{xi}	0.95	2.59	3.491(2)	159

* Symmetry codes: ^{i} $-x+1, -y+1, -z+1$; ^{ii} $x, y, z-1$; ^{iii} $-x+1, -y+1, -z$; ^{iv} $x-1, y+1, z-1$; ^{v} $x-1, y+1, z-1$; ^{vi} $x-1, y+1, z$; ^{vii} $x, y, z-1$; ^{viii} $-x+1, -y+1, -z$; ^{ix} $x, y+1, z$; ^{x} $x-1, y, z$; ^{xi} $x, y+1, z$.

		III		
C(10)–H(10)···O(3)^{i}	0.95	2.31	3.190(9)	153
C(13)–H(13)···O(2)^{ii}	0.95	2.44	3.285(7)	148
C(13)–H(13)···O(3)^{iii}	0.95	2.47	3.003(8)	115
C(15)–H(15)···O(7)^{iv}	0.95	2.52	3.194(13)	128

* Symmetry codes: ^{i} $x, y-1, z$; ^{ii} $x+1/2, y, -z$; ^{iii} $x, -y+1, z-1/2$; ^{iv} $x+3/2, -y+1, -z+1/2$.

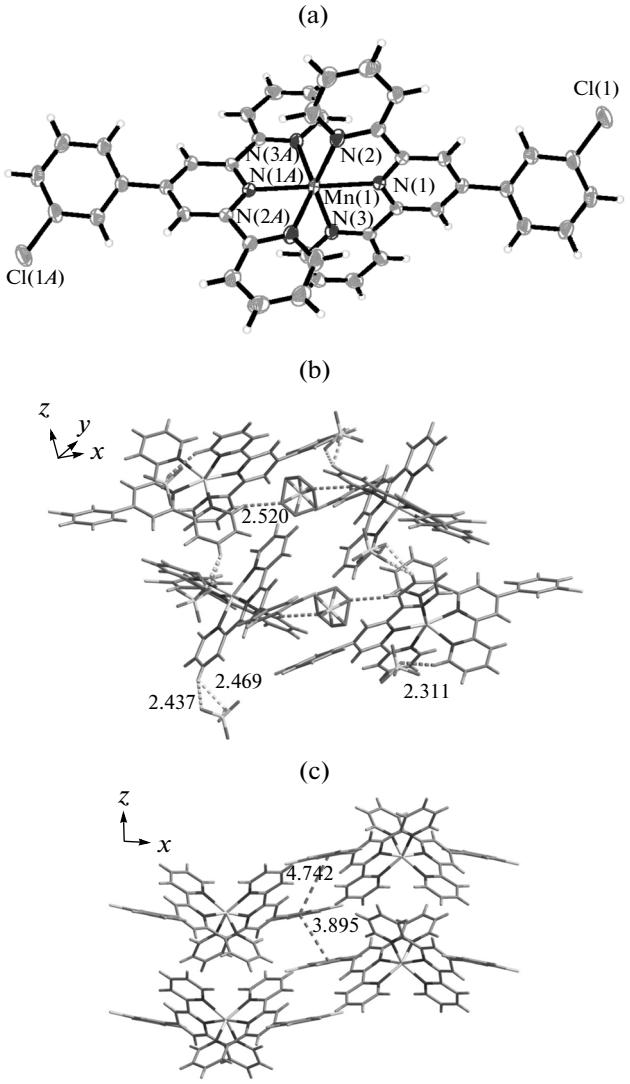

Fig. 3. The ORTEP view of $[Mn(m\text{-ClPhtpy})_2]^{2+}$ in **III** with thermal ellipsoids at 30% probability level (a); the hydrogen bonds in **III** (shown in dashed lines) (b); the face-to-face π–π interactions in **III** (shown in dashed lines) (c).

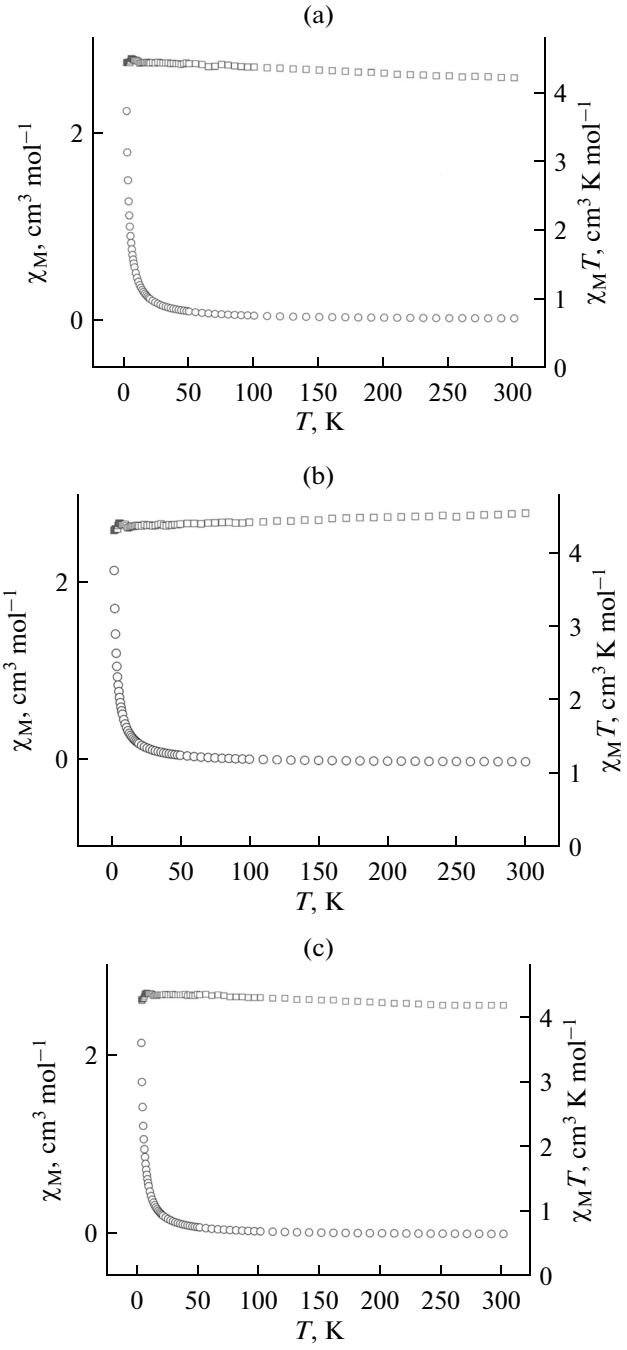

Fig. 4. Plots of χ_M (○) and $\chi_M T$ (□) *versus* T for **I** (a), **II** (b) and **III** (c) at 2–300 K.

fitting of the curve for the χ_M^{-1} *versus* T plot to the Curie–Weiss law ($\chi_M = C/(T-\theta)$], gave good results in the temperature range 2–300 K with C (θ) 4.456 (–0.016), 4.457 (–0.045) and 4.420 mol^{-1} K (–0.057 K) for **I**, **II** and **III**, respectively, showing the presence of weak antiferromagnetic interactions in **I–III** [25]. The interactions between Mn^{2+} ions were also simulated according to a single ion expression model $\chi = Ng^2\beta^2/3kTS(S+1)/\{1-(2zj'/Ng^2\beta^2)[Ng^2\beta^2/3kTS(S+1)]\}$ as the distances between Mn^{2+} ions are all longer than 7.5 Å. Between 2–300 K, g (zj') values are 2.0185 (–0.0019), 2.0186 (–0.005), and 2.0102 (–0.0067) for **I**, **II**, and **III**, respectively. The negative sign of zj' values are consistent with the negative sign of θ, showing the antiferromagnetic interaction in **I–III**. Different magnetic properties for **I–III** may be assigned to different Mn(II)–Mn(II) distances and hydrogen bonds which resulted from diverse crystal packing modes for different 4' substituted terpyridine complexes. However, the differences are rather small and different substitute show little influence on magnetic properties of terpyridine Mn(II) compounds like **I–III**.

ACKNOWLEDGMENTS

Financial support by the Key Discipline Project of Hunan Province, the Open Fund of Key Laboratory of Functional Organometallic Materials of Hunan Province College (GN14K02), and Aid program for Science and Technology Innovative Research Team in Higher Educational Institutions of Hunan Province are gratefully acknowledged.

REFERENCES

1. Alcock, N.W., Barker, P.R., Haider, J.M., et al., *Dalton Trans.*, 2000, no. 9, p. 1447.
2. Wadman, S.H., Tooke, D.M., Spek, A.L., et al., *Inorg. Chim. Acta.*, 2010, vol. 363, p. 1701.
3. Jin, X.-H., Cai, L.-X., Sun, J.-K., et al., *Inorg. Chem. Commun.*, 2010, vol. 13, p. 86.
4. Misra, P., Liao, C.-Y., Wei, H.-H., et al., *Polyhedron*, 2008, vol. 27, p. 1185.
5. Liu, P., Wong, E.L.-M., Yuen, A.W.-H., et al., *Org. Lett.*, 2008, vol. 10, p. 3275.
6. Kharat, A.N., Bakhoda, A., and Hajiashrafi, T., *J. Mol. Catal., A,* 2010, vol. 333, p. 94.
7. Kharat, A.N., Bakhoda, A., Bruno, G., et al., *Polyhedron*, 2012, vol. 45, p. 9.
8. Lee, Y.H., Kubota, E., Fuyuhiro, A., et al., *Dalton Trans.*, 2012, vol. 41, p. 10825.
9. Zhou, F.-X., Zheng, Z., Zhou, H.-P., et al., *CrystEngComm*, 2012, vol. 14, p. 5613.
10. Bhaumik, C., Das, S., Maity, D., et al., *Dalton Trans.*, 2011, vol. 40, p. 11795.
11. Beves, J.E., Constable, E.C., Housecroft, C.E., et al., *Polyhedron*, 2009, vol. 28, p. 3828.
12. Wang, X.-Y., Wei, H.-Y., Wang, Z.-M., et al., *Inorg. Chem.*, 2005, vol. 44, p. 572.
13. Zhang, X.-M., Wang, Y.-Q., Li, X.-B., et al., *Dalton Trans.*, 2012, vol. 41, p. 2026.
14. Miyasaka, H., Madanbashi, T., Saitoh, A., et al., *Chem. Eur. J.*, 2012, vol. 18, p. 3942.
15. Long, X.-J., Dai, J.-W., and Wu, J.-Z., *J. Coord. Chem.*, 2012, vol. 65, p. 316.
16. Yamazaki, H., Igarashi, S., Nagata, T., et al., *Inorg. Chem.*, 2012, vol. 51, p. 1530.
17. Guo, J., Ma, J.-F., Li, J.-J., et al., *Cryst. Growth Des.*, 2012, vol. 12, p. 6074.
18. Sun, J., Xia, E.-Y., and Yan, C.-G., *J. Coord. Chem.*, 2012, vol. 65, p. 3086.
19. Duboc, C., Collomb, M.-N., Pécaut, J., et al., *Chem. Eur. J.*, 2008, vol. 14, p. 6498.
20. Yu, M.-M., Ni, Z.-H., Zhao, C.-C., et al., *Eur. J. Inorg. Chem.*, 2007, vol. 2007, p. 5670.
21. Sheldrick, G.M., SHELXL, University of Göttingen, Germany, 1997.
22. McMurtrie, J. and Dance, I., *CrystEngComm*, 2009, vol. 11, p. 1141.
23. McMurtrie, J. and Dance, I., *CrystEngComm*, 2010, vol. 12, p. 3207.
24. Romain, S., Duboc, C., Neese, F., et al., *Chem. Eur. J.*, 2009, vol. 15, p. 980
25. Jia, Q.-X., Qian, X.-B., Wu, H.-H., et al., *Inorg. Chim. Acta*, 2009, vol. 362, p. 2213.